A Contribution on the Occasion of the 65th Birthday of Professor Władysław Rudziński

Energetic Topography in Adsorption onto Heterogeneous Surfaces

A.J. Ramirez-Pastor, F. Bulnes, M. Nazzarro, J.L. Riccardo and G. Zgrablich* *Laboratorio de Ciencias de Superficies y Medios Porosos, Universidad Nacional de San Luis, CONICET, San Luis, Argentina.*

ABSTRACT: The adsorption of gases onto heterogeneous surfaces has been reviewed, highlighting models capable of taking energetic topography effects into account. The basic ideas are contained in the fundamental Generalized Gaussian Model (GGM) developed to represent mobile adsorption onto heterogeneous surfaces at low coverage, where the energetic topography is considered through an adsorptive energy distribution with a spatial correlation function. Adsorbate molecules interact amongst them via Lennard-Jones interactions. Model predictions have been compared to Monte Carlo simulations of adsorption onto heterogeneous solids obtained by doping a pure crystalline solid with different concentrations of impurities. Energetic topography effects were shown to be important, being predicted correctly by the model at low coverage. In addition, a simplified patchwise model was also considered. The adsorption of particles with nearest-neighbour attractive and repulsive interactions was studied using Monte Carlo simulation on bivariant surfaces characterized by patches of weak and strong adsorbing sites of size "i". Patches were considered to have either a square or a strip geometry, arranged either in a deterministic ordered structure or in a random way. Quantities have been identified which scale obeying power laws as a function of the scale length "l". The consequences of this finding for the determination of the energetic topography of a surface from adsorption measurements were discussed.

1. INTRODUCTION

The role of the surface characteristics of the adsorptive in many processes of practical importance is a topic of increasing interest in surface science. Adsorption, surface diffusion and reactions on catalysts are some of the phenomena which are strongly dependent upon surface structure. Most materials have heterogeneous surfaces which, when interacting with gas molecules, present a complex spatial dependence of the adsorptive energy. It is of substantial interest to attempt a complete characterization of such heterogeneity. Although physical adsorption has been used for determining the energetic properties of heterogeneous substrates for some 50 years, the role of the surface characteristics of the adsorptive still remains an open question in many cases (Steele 1974; Jaroniec and Madey 1988; Rudziński and Everett 1992; Rudziński *et al*. 1997).

For a very long time in the history of studies of heterogeneous adsorbents, the adsorptive energy distribution (AED) was considered as the only important characteristic necessary for a description

*Author to whom all correspondence should be addressed. E-mail: giorgio@unsl.edu.ar.

of the behaviour of adsorbed particles, and much effort was dedicated to its determination by inverting the integral equation (Jaroniec and Bräuer 1986):

$$\bar{\theta}(T,\mu) = \int \theta(T,\mu,\varepsilon) f(\varepsilon) d\varepsilon \quad (1)$$

where $\bar{\theta}$ is the mean total coverage at temperature T and chemical potential μ, θ is the local coverage (usually called the local isotherm) corresponding to an adsorptive energy ε and $f(\varepsilon)$ is the AED. It should be noted that equation (1) is strictly and generally valid only for non-interacting particles, which is a quite unrealistic case. If adsorbed particles interact with each other, then the local coverage at a point with a given adsorptive energy depends on the local coverage on neighbouring points with different adsorptive energies and, in general, equation (1) should be replaced by a much more complex one, such as (Riccardo *et al*. 1992):

$$\bar{\theta}(T,\mu) = \int ... \int \theta(T,\mu,\varepsilon_1,...,\varepsilon_M) f_M(\varepsilon_1,...,\varepsilon_M)\, d\varepsilon_1 ... d\varepsilon_M \quad (2)$$

where θ now depends not only on the adsorptive energy at a single point on the surface but also on the adsorptive energy at (in general) M neighbouring points, and $f_M(\varepsilon_1,..., \varepsilon_M)$ is a multivariate probability distribution which specifies how adsorptive energies are spatially distributed, or in other words, the *energetic topography* of the surface.

It should be pointed out that, even for interacting particles, equation (2) reduces to equation (1) for two extreme topographies: (a) *random sites topography* (RST), where adsorptive energies are distributed totally at random among adsorbing sites, and (b) *large patches topography* (LPT), where the surface is assumed to be a collection of homogeneous patches sufficiently large to allow border effects between neighbouring patches with different adsorption energies to be neglected. Of course, the local adsorption isotherm will be different for these two extreme topographies. It is by now clear that RST and LPT are particular limiting cases (which occur only rarely in real systems) of heterogeneous surfaces with more general topographies, and that the topography has a strong effect on many molecular processes occurring on such surfaces, viz. adsorption, surface diffusion and chemical reactions (Riccardo *et al*. 1992; Zgrablich *et al*. 1996a,b; Bulnes *et al*. 1999a,b, 2002; Ripa and Zgrablich 1975), thus making the simple determination of the AED insufficient for characterizing the heterogeneity. It is therefore necessary to obtain the multivariate probability distribution, or at least the AED plus the spatial correlation function.

At this point, it is possible to see precisely the difficulties involved in the characterization of a general heterogeneous surface. As is well known, equation (1) — which applies to simple cases of two extreme topographies — is ill-suited for the determination of the AED $f(\varepsilon)$ due to the form of the kernel of the integral equation determined by the local isotherm. The determination of the AED from experimental adsorption isotherms requires the use of elaborate computational methods which have been developed with much effort over many years (Jaroniec and Bräuer 1986). Equation (2), where the local isotherm is a much more complex equation (if available at all), must be used when treating more general topographies, and where a multiple integral of the energy must be employed and the unknown quantity to be calculated is the multivariate adsorptive energy distribution. Even in the simplest case in which the topography may be described by a two-point correlation function, the problem cannot be solved by inverting the multi-dimensional integral equation.

It is therefore of great importance to develop simple models capable of describing the energetic topography on the basis of a few parameters and to study the effects of these parameters on several surface processes in the hope that methods to obtain the relevant parameters from the experimental data will be envisaged as a result. These models can be of two kinds: continuum models or lattice–gas models. The former are more suited to mobile adsorption (generally, physisorption) and thus more closely related to the surface energetic characterization problem, while the latter are more suited to localized adsorption (for example, chemisorption).

In the present work, we consider two kinds of theoretical approaches. Firstly, we review the Generalized Gaussian Model (a continuum model based on a bivariant energy distribution with spatial correlations), extend it to deal with particles interacting through a Lennard-Jones potential and compare its predictions to Monte Carlo simulations of mobile adsorption on solids with well-controlled heterogeneity. In Section 2, the basic concept of the *Adsorptive Energy Surface* (AES) is introduced on the basis of a simple example and the characteristics determining the topography are discussed. In Section 3, the Generalized Gaussian Model (GGM) is reviewed and extended to deal with Lennard-Jones interacting particles. A Monte Carlo simulation method to obtain adsorption isotherms for solids with well-characterized heterogeneity is then developed in Section 4. Results from simulations and from the model are presented and compared in Section 5.

Secondly, we refer to the bivariant model, a lattice–gas model based on the concept of bivariant surfaces, i.e. surfaces composed by two kinds of sites (say weak and strong sites, with adsorptive energies ε_1 and ε_2, respectively, arranged in patches of size "l"). Recent developments in the theory of adsorption on heterogeneous surfaces, such as the *supersite approach* (Steele 1999), and experimental advances in the tailoring of nano-structured adsorbates (Yang *et al*. 1998; Lopinski *et al*. 2000), encourage this kind of study. A special class of bivariant surfaces with a chessboard structure has been observed to occur recently in a natural system (Fishlock *et al*. 2000), although such an arrangement has been used extensively already in modelling adsorption and surface diffusion phenomena (Nitta *et al*. 1984, 1997; Balazs *et al*. 1991; Patrykiejew 1993; Nieto and Uebing 1998). To a rough approximation, bivariant surfaces may also mimic more general heterogeneous adsorbates. To give two examples; surfaces with energetic topographies arising from a continuous distribution of adsorptive energy with spatial correlations, such as those described by the Dual Site–Bond model (Zgrablich *et al*.1996b), or that arising from a solid where a small amount of randomly distributed impurity (strongly adsorptive) atoms are added (Bulnes *et al*. 1999a). In both cases, the energetic topography may be roughly represented by a random spatial distribution of irregular patches (of a characteristic size) of weak and strong sites.

Accordingly, the scope of the present work has been to determine, via Monte Carlo simulation, the general properties of the adsorption of interacting particles on model bivariant surfaces with a *characteristic correlation length*, l, and find out to what extent this length scale may be determined from adsorption measurements. In Section 6, we present the bivariant adsorption model and simulation method. The behaviour of relevant quantities, such as adsorption isotherms and isosteric heats of adsorption, is discussed in Section 7. Section 8 is dedicated to the determination of general scaling properties leading to power-law behaviour and to the discussion of its implications in the determination of the characteristic correlation length, l, from experimental measurements. Section 9 is devoted to an application of the model to the highly interesting case of particle adsorption with multi-site occupation. Finally, Section 10 lists the general conclusions arising from this work.

2. THE ADSORPTIVE ENERGY SURFACE (AES)

In order to base our analysis on a well-defined simple system, let us consider a heterogeneous solid consisting of a regular crystal of atoms A (for example, an hcp crystal) where a small fraction of such atoms are substituted by impurity atoms B. We move a probe atom P on the (X,Y) surface of the crystal; the probe interacts with atoms A and B with a Lennard-Jones potential:

$$U_{PS}(r) = -4\varepsilon_{PS}\left[\left(\frac{\sigma_{PS}}{r}\right)^{6} - \left(\frac{\sigma_{PS}}{r}\right)^{12}\right] \quad (3)$$

where S stands for the substrate atom, A or B, and ε and σ are the usual energy depth and particle-diameter parameters, respectively. At each point i = (X,Y), the total interaction energy of the probe atom is calculated as a function of Z by summing up all pairwise interactions with the atoms of the substrate within a cut-off distance $r_c = 4\sigma_{PS}$:

$$E(X,Y,Z) = \sum_{r_{ij} \le r_c} U_{PS}(r_{ij}) \quad (4)$$

Then, by finding the minimum in the coordinate Z, we obtain the equilibrium height Z_0 and the adsorptive energy at position (X,Y) on the surface. In this way, we obtain the *adsorptive energy surface* (AES) seen by the probe atom, defined as $E(X,Y,Z_0) = \min_z\{E(X,Y,Z)\}$.

Figure 1 shows this energy surface for a crystal containing 20% of impurity atoms with $\varepsilon_{PA}/k_B = 160$ K, $\varepsilon_{PB}/k_B = 320$ K and $\sigma_{PS} = 0.35$ nm; the darker regions represent stronger adsorptive energy, while the brighter ones correspond to weaker adsorptive energy. It will be noted that a significant correlation is present. Thus, the strong adsorptive regions appear to be significantly larger than one lattice size despite the low density of the impurity atoms, thereby reflecting the

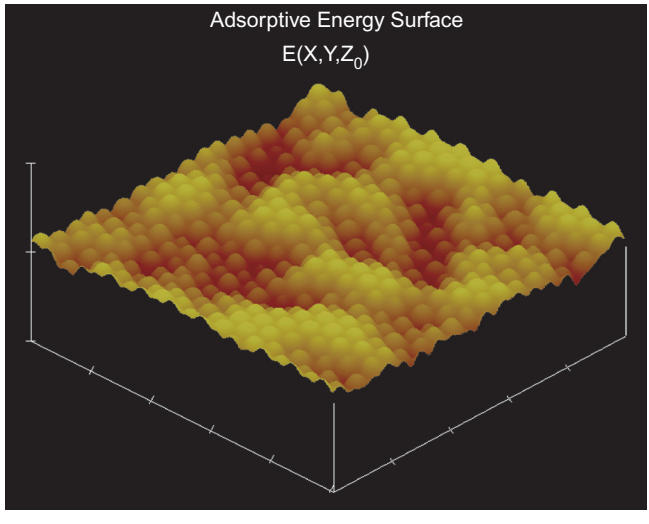

Figure 1. Adsorption Energy Surface (AES) for a crystal composed of atoms A with 20% impurity of atoms B.

fact that the probe atom interacts simultaneously with many atoms of the substrate. As a first rough approximation, the energy surface may be considered as a collection of irregular patches of different strengths. However, the energetic topography shows considerably greater complexity and such a picture could lead to an oversimplified model not reflecting important behaviours in molecular processes occurring on the surface. The slices through the borders of the sample give the adsorptive energy profiles along the X- and Y-directions, reinforcing the idea of a high complexity. This poses the problem as to how to model in a simple, but still realistic way, such complex behaviour? In other words, which are the characteristic (and relevant) quantities necessary to construct simple models capable of reproducing the main topographic features in a statistical sense?

In a very general way, we can say that the AES is mathematically described by a stochastic process (Gardiner 1985; Hill 1956), i.e. a random function depending on some parameter. In our case, the adsorptive energy is a random function of the position on the surface, $\hat{E}(\vec{R})$, where the symbol (^) indicates a random quantity and $\vec{R}$ is the position vector on the surface whose components are (X,Y). A particular realization of the stochastic process $\hat{E}(\vec{R})$ is the function E(X,Y) represented in Figure 1 (the dependence upon Z_0 may be ignored). The statistical description of such a stochastic process could be very complex. However, some simplifying assumptions, based on physical grounds, may greatly reduce this complexity. In fact, it is reasonable to assume that the surface is statistically homogeneous, i.e. any macroscopic portion of the surface possesses all the meaningful information, and that the adsorptive energy distribution can be approximately described by a multivariate Gaussian distribution depending on the distance between pairs of points on the surface. This approach leads to the *Generalized Gaussian Model* (GGM) (Riccardo *et al*. 1992; Ripa and Zgrablich 1975) which is capable of describing the energetic topography on the basis of the mean and the dispersion of the adsorptive energy, and a correlation function depending on the distance on the surface.

3. GENERALIZED GAUSSIAN MODEL (GGM)

The GGM was introduced and developed (Riccardo *et al*. 1992; Ripa and Zgrablich 1975) for particles interacting through a square-well potential. Here, we review briefly the main formulation of the model and calculate adsorption isotherms corresponding to particles interacting through a Lennard-Jones potential. The model is based on a Gaussian multivariate probability density distribution (Feller 1971; Gardiner 1985) for the adsorptive energies at n points on the surface given by:

$$\begin{aligned}\Phi_n(E_1,...,E_n) &\equiv \left\langle \prod_{i=1}^{n} \delta[\hat{E}(\vec{R}_i) - E_i] \right\rangle \\ &= [(2\pi)^n \det H]^{-1} \exp\left[-\frac{1}{2} \sum_{i,j=1}^{n} (E_i - \bar{E})(H^{-1})_{i,j}(E_j - \bar{E}) \right] \end{aligned} \tag{5}$$

where the covariance matrix:

$$H_{i,j} = \left\langle (E_i - \bar{E})(E_j - \bar{E}) \right\rangle = \Omega^2 C(\vec{R}_i - \vec{R}_j) \tag{6}$$

is a function of the relative position vector between two points. Here Ω is the adsorptive energy dispersion and C the correlation function. If the surface is statistically isotropic, C is only a function of the distance r between two points.

In this model, the mean value of any macroscopic quantity of interest depending on the AES could then be evaluated by knowing $\bar{E}$, Ω and C(r). The correlation function C(r) carries all the useful information about the energetic topography and should, in principle, be determined from the geometric and chemical structure of the adsorbent (even though the methodology to achieve this has not been developed so far). However, we could simplify the model even more by proposing for C(r) a simple Gaussian decay as:

$$C(r) = \exp\left[-\frac{1}{2}\left(\frac{r}{r_0}\right)^2\right] \tag{7}$$

where r_0 is a *correlation length*. This expression, which we do not intend to take as a realistic correlation function valid for any surface, simply stresses that the spatial correlation between adsorptive energies at points separated by a distance $r < r_0$ is very high (close to 1) while for $r > r_0$ it is very low (close to zero). Thus, the present model becomes very attractive in the sense that the energetic topography is characterized by a single parameter, the correlation length, and this opens the possibility for determining the three simple parameters of the model ($\bar{E}$, Ω and r_0) by, for example, fitting experimental adsorption isotherms. It is worth remarking that the present model is a continuous one and not a lattice model of adsorption sites. This is an appealing feature, since, as we can see from Figure 1, adsorption sites hardly form a regular lattice and furthermore many of them are so shallow that an adsorbed particle will most probably be quite mobile on appreciably large regions.

The adsorption isotherm is obtained as a virial gas–solid expansion (Hill 1956) in density in the form:

$$P = K(T)\rho\exp\left[\sum_{n\geq 2}\frac{n}{n-1}B_n(T)\rho^{n-1}\right] \tag{8}$$

where ρ is the adsorbate surface density, $B_n(T)$ is the nth two-dimensional virial coefficient and K(T) is a constant. By assuming that the potential energy of the system of adsorbed particles is the sum of the inter-particle potential $U_{gg}\left(\left|\vec{R}_i - \vec{R}_j\right|\right)$ and the gas–solid potential (Steele 1974)

$$U_{gs}(\vec{R},Z) = \tfrac{1}{2}k_z(Z - Z_0)^2 + \hat{E}(\vec{R}) \tag{9}$$

and that the stochastic process $\hat{E}(\vec{R})$ has the distribution given by equation (5), then the coefficients in equation (8) are obtained as (Ripa and Zgrablich 1975):

$$K(T) = (k_B T k_z/2\pi)^{1/2}\exp\left[\frac{\bar{E}}{k_B T} - \frac{1}{2}\left(\frac{\Omega}{k_B T}\right)^2\right] \tag{10}$$

$$B_n(T) = -\frac{1}{n(n-2)!}\int\cdots\int d\vec{R}_1\ldots d\vec{R}_n\,\delta(\vec{R}_1+\ldots+\vec{R}_n)\,S'_{1,\ldots,n}\prod_{i>-j=1}^{n}\exp\left[\left(\frac{\Omega}{k_B T}\right)^2 C(\vec{R}_i - \vec{R}_j)\right] \tag{11}$$

where

$$S'_{1,2} = f_{12} = \exp\left[-U_{gg}\left(\left|\vec{R}_i - \vec{R}_j\right|\right)/k_BT\right] - 1$$

$$S'_{1,2,3} = f_{12}f_{13}f_{23}$$

$$S'_{1,2,3,4} = f_{12}f_{13}f_{14}f_{23}f_{24}f_{34} + 6f_{12}f_{13}f_{14}f_{23}f_{34} + 3f_{12}f_{23}f_{34}f_{14}$$

and so on. It is clear that the calculation of gas–solid virial coefficients is very difficult so that only the first few of them may be evaluated. This means that the model will be useful only at low values of the adsorbed-phase density. On the other hand, however, the most important effects of heterogeneity can be seen for the low-pressure part of the adsorption isotherm.

In order to study how the first few virial coefficients depend on the energetic topography, we assume an inter-particle interaction given by a Lennard-Jones potential:

$$U_{gg}(r) = 4k_BT_{gg}\left[\left(\frac{\sigma}{r}\right)^{12} - \left(\frac{\sigma}{r}\right)^{6}\right] \tag{12}$$

where σ is the particle diameter and k_BT_{gg} is the depth of the potential. Detailed calculations of B_2 and B_3 have been reported elsewhere (Nazzarro and Zgrablich 2003).

Adimensional virial coefficients can be defined as $B'_n = B_n/(\pi\sigma^2/2)^n$. Using the notation $\bar{E} = -k_BT_a$ and $\Omega = k_BT_s$, the second and third coefficients are shown in Figure 2 as a function of T/T_{gg} for $T_s/T_{gg} = 2.0$ (which represents a reasonably high heterogeneity with respect to inter-particle interactions) and different values of r_0. As can be seen from the data depicted in the

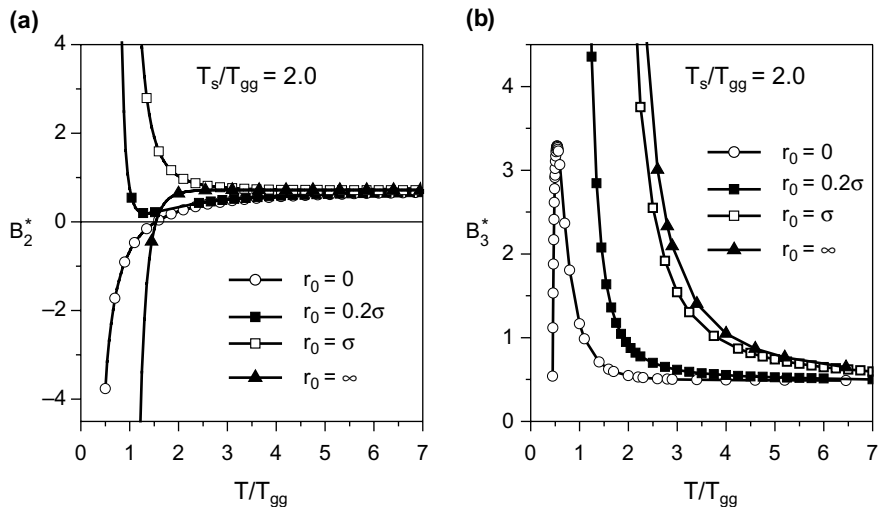

Figure 2. Normalized gas–solid virial coefficients, (a) B_2^* and (b) B_3^*, for a Lennard-Jones potential as a function of the reduced temperature T/T_{gg}, for different values of the correlation length r_0 and for a given value of the standard deviation of the adsorptive potential k_BT_s.

figure, the sensitivity of the virial coefficients with respect to the correlation length r_0 is very high at low temperature and still appreciable even at relatively high temperature. As T_s/T_{gg} decreases (figures not shown here), the effect of topography becomes weaker and virtually disappears for $T_s/T_{gg} < 0.5$. It is interesting to analyze the adsorption process to understand the peculiar behaviour of B_2 at low temperature. For $r_0 = 0$ (completely random topography) and $r_0 \to \infty$ (macroscopic homogeneous patches), the relative positions of adsorbed particles is not dictated by the adsorption energy topography but rather by the interparticle potential, with a prevalence of the attractive region, thus making $B_2 \to +\infty$ as $T \to 0$. In contrast, for $0 < r_0 < 2\sigma$, adsorbed particles are forced by the adsorptive energy topography to be sufficiently close that the repulsive part of the interparticle potential is dominant and $B_2 \to -\infty$ as $T \to 0$. Thus, virial coefficients for r_0 greater than a few particle diameters will behave approximately as for $r_0 = \infty$.

Once the virial coefficients have been evaluated, the adsorption isotherm for low pressure is obtained via:

$$P = K(T)\rho \exp\left[2B_2(T)\rho + \tfrac{3}{2}B_3(T)\rho^2\right] \tag{13}$$

$$K(T) = \left(k_B T k_z/2\pi\right)^{1/2} \exp\left[-T_a/T - \tfrac{1}{2}\left(T_s/T\right)^2\right] \tag{14}$$

The constant K(T), known as the Henry constant, representing the slope of the adsorption isotherm at very low pressure, depends not only on the mean adsorptive energy, $\bar{E} = -k_B T_a$, as believed classically (Rudzinski and Everett 1992), but also on the adsorptive energy dispersion $\Omega = k_B T_s$.

Adsorption isotherms calculated from the above equations for $T_s/T_{gg} = 2$, $T/T_{gg} = 2$ and different values of the correlation length r_0 are shown in Figure 3. The effect of the correlation length is clearly shown as a considerable decrease in the adsorption density as r_0 increases. Theoretical

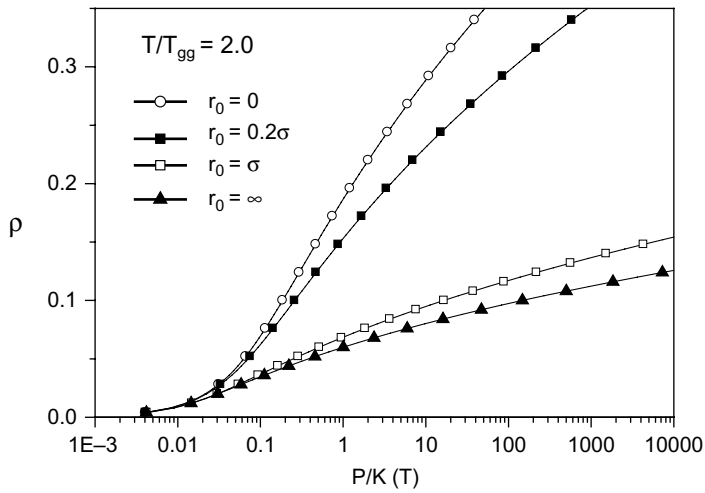

Figure 3. Adsorption isotherms calculated from the GGM for Lennard-Jones interacting particles, for $T/T_{gg} = 2.0$ and different values of the correlation length.

adsorption isotherms could be fitted to the experimental ones to obtain the parameters K(T), T_s and r_0 characterizing the adsorptive energy surface for a given real gas–solid system. In what follows, however, we point to a quite stronger test of the GGM. Thus, we produce artificial (computer-generated) heterogeneous adsorbents with well-controlled energetic topographies, determine the AEDs and correlation functions corresponding to the gas–solid system concerned, then simulate the adsorption process in the continuum and finally compare the observed behaviour with the *predictions* (not data-fitting) of the GGM.

4. SIMULATIONS ON IDEAL HETEROGENEOUS SYSTEMS

A collection of solids is prepared as explained in Section 2, corresponding to different concentrations of impurity atoms, and their AES values generated. We can then study the statistical properties of these AES values in the same manner as the AED and the spatial correlation function C(r). These statistical properties for a set of ideally prepared heterogeneous solids are shown in Figures 4 and 5. As the concentration of impurity atoms increases, the mean value of the adsorption energy distribution (Figure 4) shifts toward lower energy values (stronger adsorption) and its dispersion also increases. At the same time, the spatial correlation function (Figure 5) presents an attenuated oscillatory behaviour, decaying slower for higher concentrations of impurity atoms.

Once the ideal heterogeneous solids are prepared, the adsorption process is simulated through a continuum space Monte Carlo method in the Grand Canonical ensemble (Binder 1986; Nicholson and Parsonage 1982).

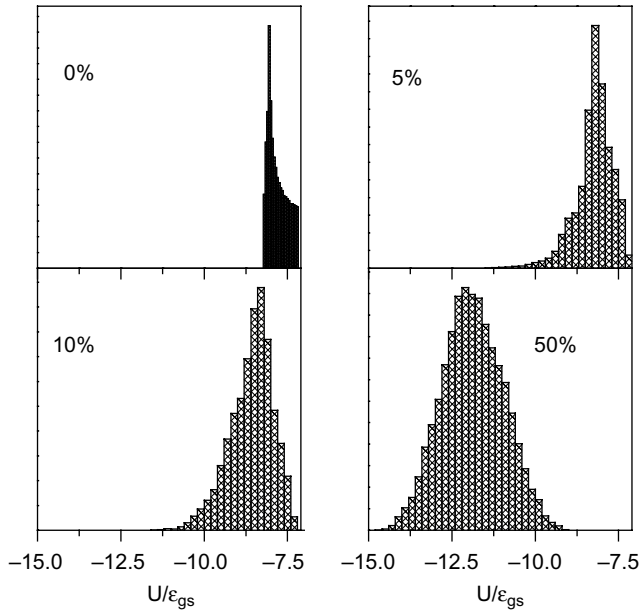

Figure 4. Adsorptive energy distributions (AEDs) for ideal heterogeneous solids with different concentrations of impurity atoms as indicated.

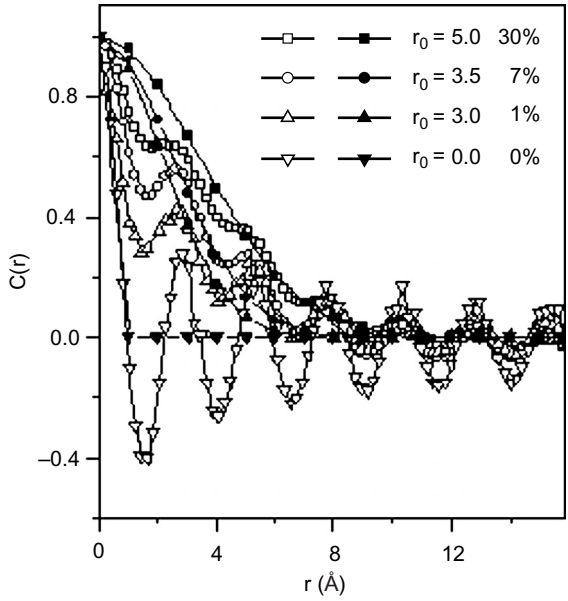

Figure 5. Comparison between "real" spatial correlation functions (shown by open data symbols) and those assumed by the GGM (shown by filled data symbols).

5. COMPARISON TEST FOR THE GGM

We now compare the predictions of the GGM with the behaviour observed through simulations for ideal heterogeneous systems

As can be seen from Figure 4, the adsorptive energy distribution may be qualitatively described by a Gaussian distribution, as assumed by the GGM, whose dispersion increases as the concentration of impurity atoms increases. The case corresponding to 0% concentration of impurity atoms is the least favourable, but it is also true that a distortion of the AED in the high-energy region (weak adsorption energy) is not important for adsorption at low pressure where the deeper adsorptive energy regions are preferentially occupied by adsorbed particles. For more general heterogeneous solids, where the heterogeneity could be due not only to impurity atoms but also to a number of defects or even the presence of amorphous structures, the AEDs would be expected to be even more similar to a Gaussian distribution.

The Gaussian decay assumed by the GGM is also qualitatively acceptable for the spatial correlation function, as can be seen from Figure 5 where the filled symbols represent the Gaussian decay for different correlation lengths while the open symbols represent the spatial correlation function obtained from the AES for different concentrations of impurity atoms. In fact, even if the "real" correlation function presents an oscillatory structure induced by the periodic character of the solid lattice, these oscillations are not relevant to the adsorption of molecules whose sizes are usually larger that the solid lattice spacing. What is important is the attenuation of the oscillations. Visual inspection of Figure 1 suggests the importance of the sizes of the dark and bright regions, rather than the small grains within these regions. Hence, the important fact is that the GGM provides a simple correlation function which takes into account such a decay involving only one parameter, i.e. the correlation length r_0.

TABLE 1. Parameter Values Used in the GGM to Obtain the Adsorption Isotherms Depicted in Figure 7

Concentration of impurities (%)	r_0	k_BT_a	k_BT_s	T_s/T_{gg}
1	2.0	2.76	0.10	0.20
7	2.5	2.85	0.16	0.32
30	3.5	3.49	0.32	0.64

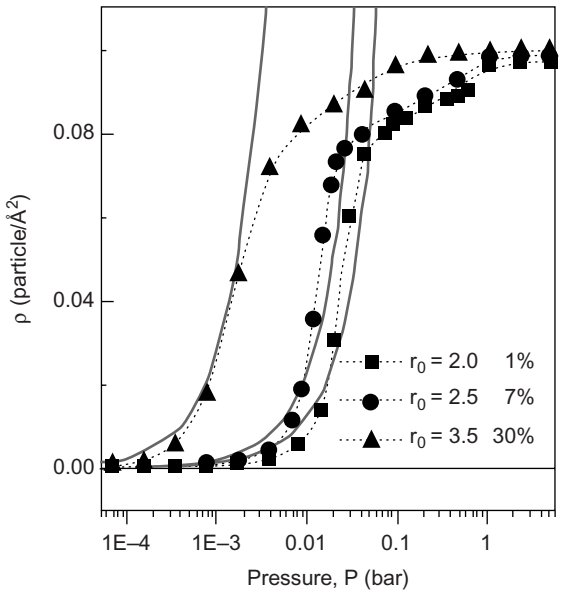

Figure 6. Comparison between adsorption isotherms simulated on ideal heterogeneous solids (black symbols) and those predicted by the GGM (dotted lines) for three different samples.

We now choose (by visual comparison) more or less appropriate AEDs and correlation length values for different samples of heterogeneous solids, as indicated by the parameters listed in Table 1, and compare the adsorption isotherms obtained by the GGM with the simulated isotherms for these samples. This comparison is shown in Figure 6, where the filled symbols represent simulated isotherms while the full curves represent the GGM predictions. As already mentioned above, such a comparison can only have significance at low pressure given that only the virial expansion up to the third coefficient is employed. The data depicted indicate that, considering that this is not the result of a parameter-fitting procedure, the predictions of the model are satisfactory in this region.

6. BIVARIANT MODEL AND SIMULATION METHOD

We now turn to a completely different kind of approach. We assume that the substrate is represented by a two-dimensional square lattice consisting of adsorption sites, with periodic

boundary conditions. Each adsorption site can be either a "weak" site with an adsorptive energy ε_1, or a "strong" site with an adsorptive energy ε_2 ($\varepsilon_1 < \varepsilon_2$). Weak and strong sites form patches of different geometry:

1. Square patches of size l (l = 1, 2, 3, ...), which are spatially distributed either in a deterministic alternate way [chessboard topography — see Figure 7(a)], or in a non-overlapping random way [random topography — see Figure 7(b)].
2. Strips of transversal size l (l = 1, 2, 3, ...), which are spatially distributed either in an ordered alternate way [Figure 7c)], or in a non-overlapping random way [random topography — Figure 7(d)].

In order to readily identify a given topography, we introduce the notation "l_C" for a chessboard topography of size "l" and, similarly, "l_R" for random-square patches, "l_{OS}" for ordered strips and "l_{RS}" for random strips. Thus, in Figures 7(a)–(d), the topographies are 4_C, 4_R, 4_{OS} and 4_{RS}, respectively. We also use the notation "bp" to refer to the extreme case of the topography of big patches ($l \to \infty$), i.e. a surface consisting of one-half weak sites and one-half strong sites.

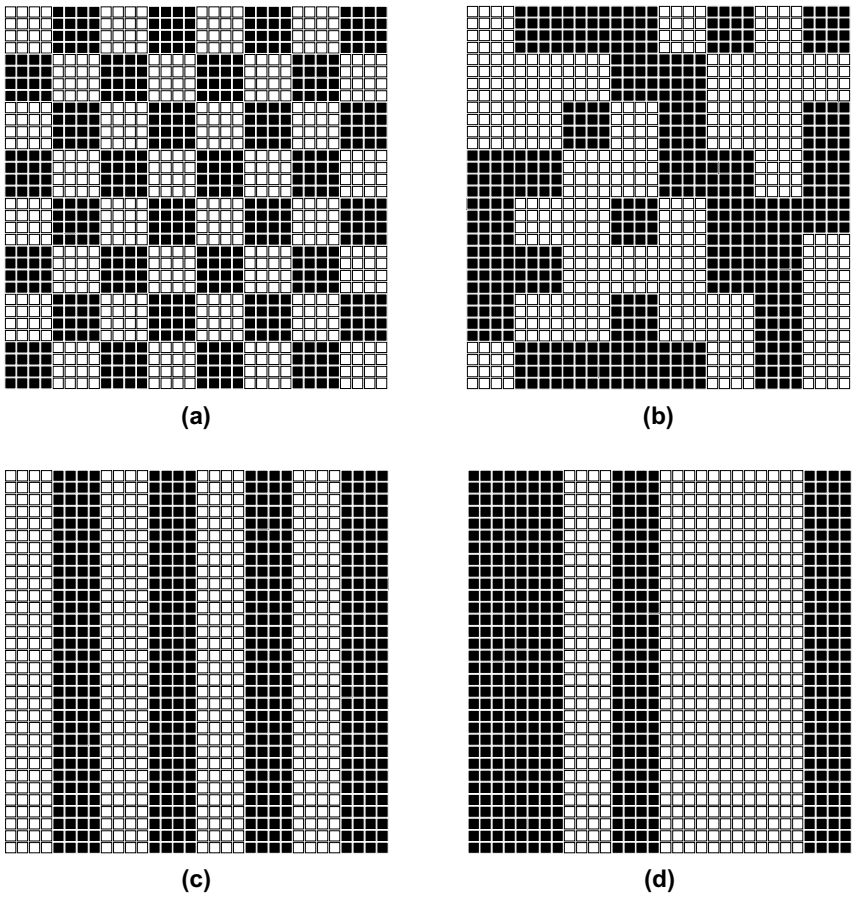

Figure 7. Schematic representation of heterogeneous bivariant surfaces with a chessboard arrangement: (a) random-square patches; (b) ordered strips; (c) random strips, (d) overall topography. The patch size in this figure is l = 4.

The substrate is exposed to an ideal gas phase at temperature T and chemical potential μ. Without any loss of generality, it is possible to consider that all energies are measured in units of k_BT and that $\varepsilon_1 = 0$ and $\varepsilon_2 = \varepsilon_1 + \Delta E$, in such a way that the adsorptive energy is characterized by the single adimensional parameter ΔE. The adsorption process is simulated through a Grand Canonical Ensemble Monte Carlo (GCEMC) method (Binder 1986; Nicholson and Parsonage 1982). Mean values of thermodynamic quantities such as the surface coverage, θ, and the internal energy, U, may be obtained by simple averaging over uncorrelated configurations, while the differential heat of adsorption, q_d, as a function of the coverage is calculated from $q_d = \partial \langle U \rangle / \partial \theta$ (Bakaev and Steele 1992).

7. ADSORPTION RESULTS

The cases of repulsive and attractive interactions are treated separately below in Sections 7.1 and 7.2, respectively.

7.1. Repulsive interactions

Since all energies are measured in units of k_BT, the results obtained will be independent of the temperature and, furthermore, since the critical temperature for the appearance of a c(2 × 2) ordered phase in a zero-field Ising model is given by $k_BT_0 = 0.567w$ (Yeomans 1992), there will be a critical NN interaction $w_0 = 1.763668$ above which the formation of the ordered phase is possible at θ = 0.5.

In order to understand the basic phenomenology, we firstly consider a chessboard topography with l = 4 (the size of each homogeneous patch). Figure 8(a) shows the behaviour of the

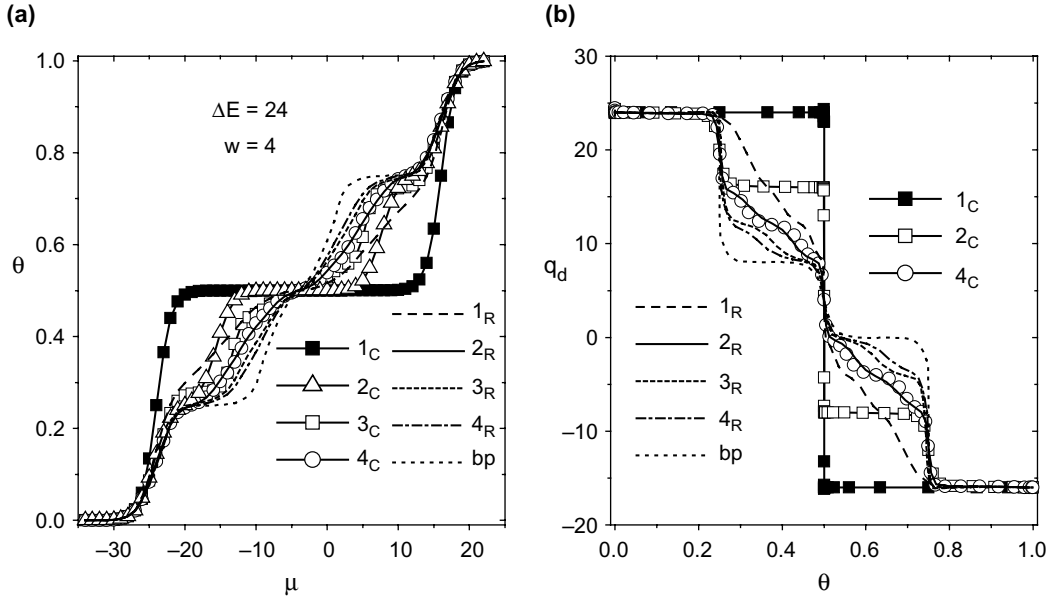

Figure 8. (a) Adsorption isotherms and (b) differential heats of adsorption for different topographies and repulsive interactions in Regime I.

adsorption isotherms while Figure 8(b) shows that of $q_d(\theta)$ for different square-patches topographies for w = 4 and $\Delta E = 24$. It will be seen that all the curves are contained between two limiting curves: one corresponding to 1_C and the one corresponding to bp. For chessboard topographies, four different adsorption processes can be visualized, separated by shoulders in the adsorption isotherm and by steps in q_d: (i) strong-site patches are filled first up to $\theta = 0.25$, where a $c(2 \times 2)$ structure is formed on them (in this region $q_d = 24$); (ii) since $4w < \Delta E$, the filling of strong-site patches is completed up to $\theta = 0.5$ (in this region q_d decreases continuously from 24 while zero-occupied NN increase to 8 four-occupied NN); processes (iii) and (iv) corresponding to the regions $0.5 < \theta > 0.75$ and $0.75 < \theta > 1$, respectively, are equivalent to processes (i) and (ii) for weak-site patches. Random topographies are seen to behave in a similar manner with a particularly interesting feature: the behaviour of a random topography of size l seems to approach that of a chessboard topography with an effective size $l_{eff} > l$. As can be easily understood, as long as the condition $w/\Delta E \leq 1/4$ is satisfied, the adsorption process is similar to the one described above, i.e. strong-site patches are filled first and weak-site patches are subsequently filled. We call this feature *Regime I*.

Figure 9(a) shows the behaviour of the adsorption isotherms and Figure 9(b) that of $q_d(\theta)$ for different square-patches topographies for w = 4 and $\Delta E = 12$. In this case, where $w/\Delta E \geq 1/3$, the adsorption process follows a different regime which we call *Regime II*: (i) the strong-site patches are filled until the $c(2 \times 2)$ ordered phase is formed on them; (ii) the weak-site patches are filled until the $c(2 \times 2)$ ordered phase is formed on them; (iii) filling of the strong-site patches is completed; (iv) filling of the weak-site patches is completed.

It should be noticed that Regimes I and II are disconnected. In between, i.e. $1/4 < w/\Delta E < 1/3$, the system behaves as a mixed transition regime changing continuously from one to the other.

Strip topography presents a similar behaviour to that of square-patches topography (not shown here), with the feature that ordered strips behave like chessboard square patches with a higher l_{eff}

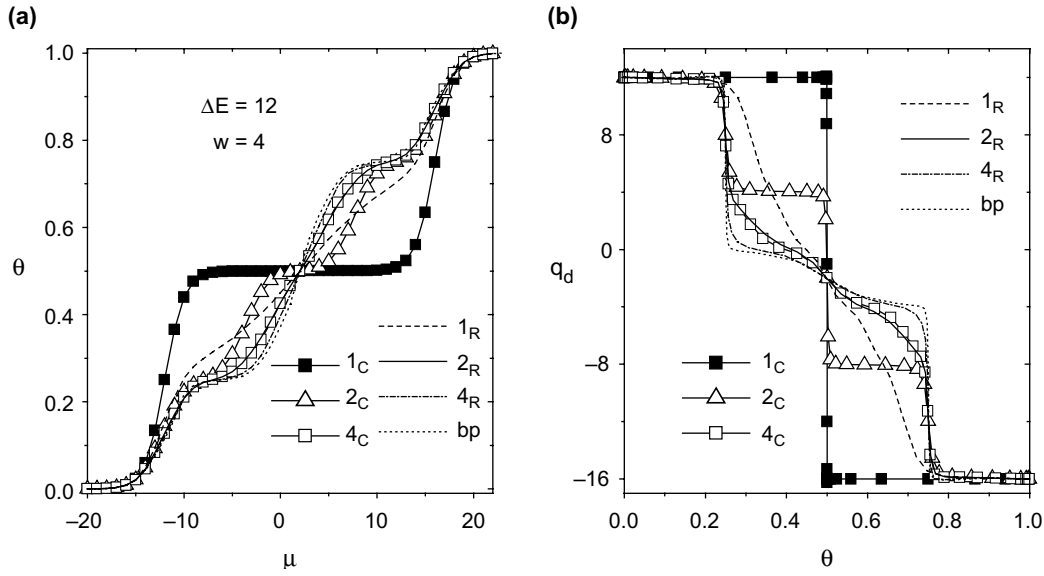

Figure 9. (a) Adsorption isotherms and (b) differential heats of adsorption for different topographies and repulsive interactions in Regime II.

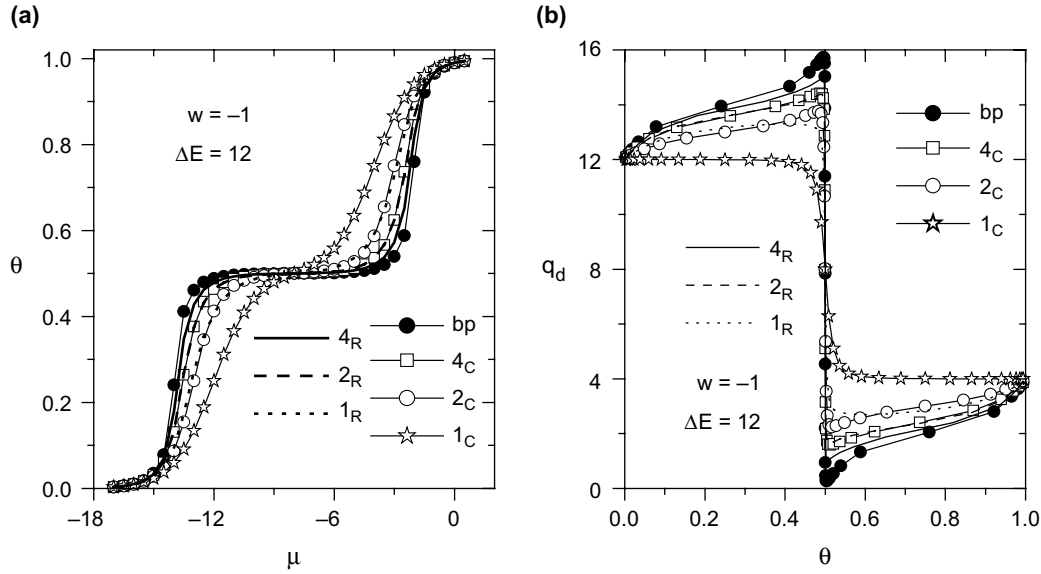

Figure 10. (a) Adsorption isotherms and (b) differential heats of adsorption for square-patches topographies and attractive interactions.

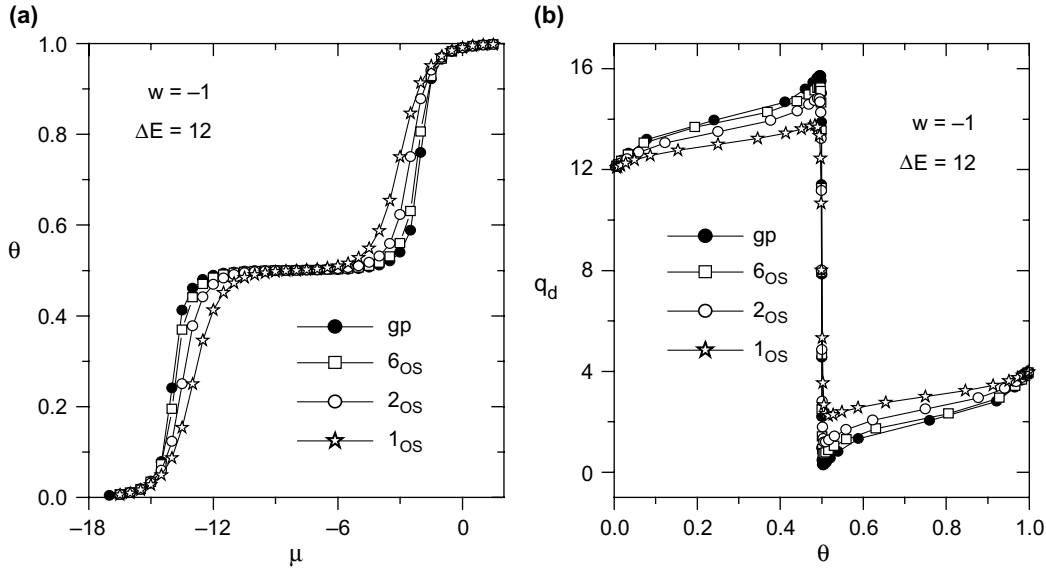

Figure 11. (a) Adsorption isotherms and (b) differential heats of adsorption for strips topographies and attractive interactions.

and random strips behave like random-square patches also with a higher l_{eff}. A more detailed description of the behaviour of the adsorption isotherms and differential heats of adsorption can be found elsewhere (Bulnes *et al*. 2001, 2002).

7.2. Attractive interactions

Only Regime I is possible for the case of attractive interactions, i.e. for all values of ΔE and w strong patches fill first and weak patches fill last. Figures 10 and 11 illustrate the typical behaviour observed for square patches and for strips, respectively. Only the ordered-strips topography has been represented in the latter case, since the density of the curves is already high. The plateau in the isotherms and the corresponding abrupt drop in the differential heat of adsorption indicate that the strong patches are being filled before adsorption starts on the weak patches. Again, we observe that all curves vary between the bp topography and the 1_C topography and that random topographies behave like the ordered ones with a larger effective size.

8. SCALING BEHAVIOUR AND TEMPERATURE DEPENDENCE

The fact that both the adsorption isotherms and heat of adsorption curves for different topographies characterized by a length scale l vary between two extreme curves suggests that we should search for some appropriate quantity to measure de-deviation among these curves and study the behaviour of such a quantity as the length scale is varied.

The most suitable quantity we have found is the area between a given curve and a reference curve. For adsorption isotherms, this quantity, χ_a, is defined as:

$$\chi_a = \int_{-\infty}^{\infty} \left| \theta(\mu) - \theta^R(\mu) \right| d\mu \tag{15}$$

where $\theta^R(\mu)$ is the reference adsorption isotherm. A similar quantity, χ_h, can be defined for the adsorption heat curves. This quantity is related to the difference in free energy arising between the filling processes for the two involved surfaces and therefore leads to a physical interpretation of the scaling behaviour (Bulnes *et al*. 2007).

By taking as a reference isotherm the one corresponding to the bp topography, we find that, for a given adsorption regime, the functions χ collapse onto a single curve for any topography when represented in terms of an *effective length scale* (representing an effective patch size), l_{eff}, given by:

$$l_{eff} = \sigma l \tag{16}$$

where σ = 1 for chessboard topography, σ = 2 for random-square patches and for ordered strips, and σ = 4 for random strips. These values of χ have been calculated analytically by Bulnes *et al*. (2002). Figure 12 shows how simulation data for the function χ lie on a single curve for Regime I when the effective length scale is used. In general, it is found that χ obeys a power law in l_{eff} of the form:

$$\ln \chi = \text{const} + \alpha \ln l_{eff} \tag{17}$$

This scaling behaviour is found to hold over the whole range of energy, with different values of the exponent α given by:

$$\begin{aligned} \alpha &= \alpha_1 = -0.976 \pm 0.053 \quad \text{for} \quad w/\Delta E \le 1/4 \\ \alpha &= \alpha_2 + [12(1/3 - w/\Delta E)]^{\beta} (\alpha_1 - \alpha_2) \quad \text{for} \quad 1/4 \le w/\Delta E \le 1/3 \\ \alpha &= \alpha_1 = -1.525 \pm 0.065 \quad \text{for} \quad w/\Delta E \ge 1/3 \end{aligned} \tag{18}$$

with β = 0.42 ± 0.04.

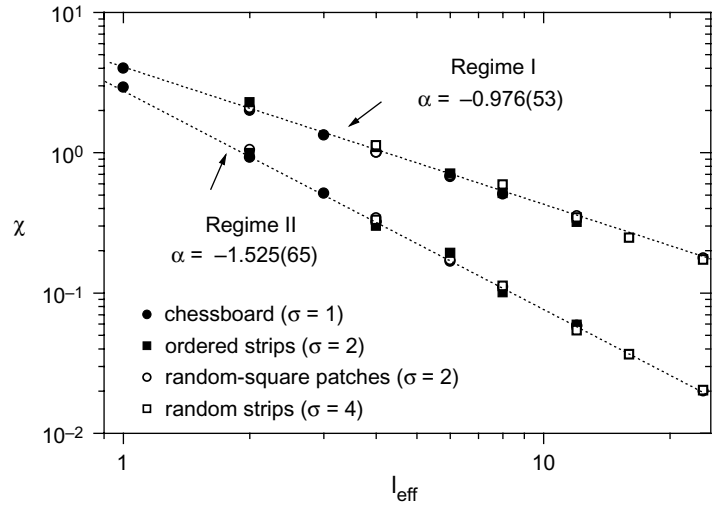

Figure 12. Power-law behaviour of the quantity χ showing the collapse of data for different topographies onto a single curve when the effective length scale l_{eff} is used for repulsive interactions.

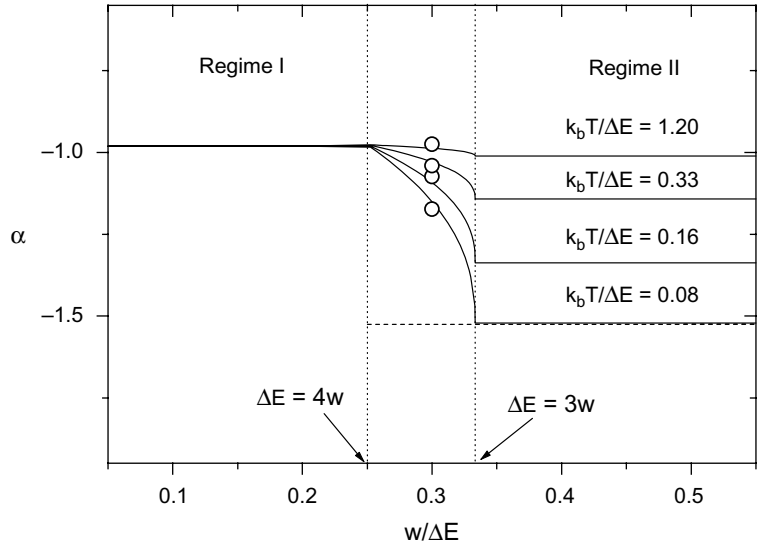

Figure 13. Universal behaviour of the exponent α as a function of the adimensional variable $w/\Delta E$ and its dependence upon the temperature.

It should be noted that in the case of attractive interactions, $w < 0$, only Regime I is possible and the value of exponent α is given by α_1 over the whole energy range.

As the temperature is changed, the scaling exponent does not change for Regime I, while for Regime II its value approaches that corresponding to Regime I as temperature increases, in the form (Romá *et al*. 2003):

$$\alpha_2 (k_B T/\Delta E) = -1 - 0.806 \exp(-5.2174 k_B T/\Delta E) \quad (19)$$

Simulations have shown that this variation with temperature is also approximately valid in the intermediate range between Regimes I and II; hence equations (18) and (19) give the general behaviour of α over the whole energy range and for all temperatures. This behaviour is shown in Figure 13.

It is important to remark that the scaling exponent α presents *universality properties* in the sense that its behaviour and value are identical for different degrees of heterogeneity, ΔE, different topographies, different reference curves (even a theoretical reference curve such as, for example, the mean field solution corresponding to bp) and for a definition of χ involving the function $q_d(\theta)$ instead of the function $\theta(\mu)$.

9. MULTI-SITE ADSORPTION ON PATCHWISE BIVARIANT SURFACES

Whilst the adsorption of monomers (particles occupying only one adsorption site) is sensitive to the energetic topography only in that case where interparticle interactions are present, the adsorption of k-mers (particles occupying k adsorption sites) is sensitive to the topography even in the absence of lateral interactions.

For the adsorption of non-interacting dimers on chessboard and random-square patches bivariant surfaces (González and Ramirez-Pastor 2002), the same scaling behaviour is found as for monomers in Regime I (this is the only possible regime for non-interacting dimmers), with the same exponent and the same universality properties. It is expected that the inclusion of interactions (especially in the case of repulsive interactions) will give rise to a rich variety of behaviours and this will be the subject of future investigations.

10. CONCLUSIONS

Several conclusions can be drawn from the present contribution. On the one hand, the mobile adsorption of gases onto heterogeneous surfaces at low pressure (i.e. more suited to physical adsorption) has been addressed. The importance of the adsorptive energy topography — which can be taken into account by a theoretical model such as the GGM — has been stressed and such a model has been extended by calculating the second and third gas–solid virial coefficients for particles interacting through a Lennard-Jones potential. Due to its simplicity, the GGM turns out to be quite an attractive model; in fact, in this model, the adsorptive energy surface is statistically described by only three parameters, viz. the mean value of the adsorptive energy distribution, $k_B T_a$, and its dispersion, $k_B T_s$, and the correlation length, r_0. This last parameter is the most relevant for describing the topography. The gas–solid virial coefficients were shown to depend strongly on the topography and, consequently, so does the adsorption isotherm at low pressure.

The only way to test the validity of such a model is to compare its predictions with the behaviour of a system whose adsorptive energy surface properties are well specified. This is the case when adsorption is simulated on ideally constructed heterogeneous solids, as has been undertaken here. The test turned out to be satisfactory for adsorption at low pressure. From the above, it may be stated that the present form of the GGM can be used to fit experimental adsorption isotherms of physically adsorbed gases on heterogeneous solids at low pressure, thereby allowing the parameters characterizing the heterogeneity to be obtained. We may expect that the model would work better with substrates presenting a rough AES, either due to chemical impurities or to roughness in the

physical surface, such as in the case of activated carbons. Finally, since virial coefficients are found to be more sensitive to the correlation length at lower temperature, the appropriate adsorbates should be selected in such a way as to obtain experimental low-density adsorption isotherms at the lowest possible temperatures, thereby ensuring good sensitivity in the fitting parameters.

Using Monte Carlo simulations, we have also studied the adsorption of particles interacting through an NN interaction, w, on heterogeneous bivariant surfaces characterized by different energetic topographies. The heterogeneity was determined by two parameters: the difference of adsorptive energy between strong and weak sites, ΔE, and an effective correlation length, l_{eff}, representing the length scale for homogeneous adsorptive patches.

Unique scaling properties and power-law behaviours have been established for relevant adsorption quantities, such as the adsorption isotherm and the differential heat of adsorption. Two distinct filling regimes, Regime I and Regime II, separated by an intermediate mixed regime, may be clearly identified in the adsorption process. The scaling exponent α as a function of $w/\Delta E$ was found to follow a universal behaviour. Its value was constant with temperature for Regime I, while it increased with temperature for Regime II and in the intermediate regime towards the value corresponding to Regime I. This temperature dependence is given as an empirical equation obtained by Monte Carlo data-fitting. These findings provide for the first time a method for characterizing the energetic topography (i.e. obtaining the parameters from experimental measurements) of a class of heterogeneous surfaces which can be approximately represented as bivariant surfaces.

ACKNOWLEDGMENTS

We gratefully acknowledge financial support from CONICET of Argentina which made the development of the present research possible.

REFERENCES

Bakaev, V. and Steele, W.A. (1992) *Langmuir* **8,** 148.
Balazs, A.C., Gempe, M.C. and Zhou, Z. (1991) *Macromolecules* **24,** 4918.
Binder, K. (1986) *Monte Carlo Methods in Statistical Physics*, Springer-Verlag, Berlin, West Germany.
Bulnes, F., Nieto, F., Pereyra, V., Zgrablich, G. and Uebing, C. (1999a) *Langmuir* **15,** 5990.
Bulnes, F., Pereyra, V., Riccardo, J.L. and Zgrablich, G. (1999b) *J. Chem. Phys.* **111,** 1.
Bulnes, F., Ramirez-Pastor, A.J. and Zgrablich, G. (2001) *J. Chem. Phys.* **115,** 1513.
Bulnes, F., Ramirez-Pastor, A.J. and Zgrablich, G. (2002) *Phys. Rev. E* **65,** 31 603.
Bulnes, F., Ramirez-Pastor, A.J. and Zgrablich, G. (2007) *Langmuir* **23,** 1264.
Feller, W. (1971) *An Introduction to Probability Theory and its Applications*, Wiley, New York.
Fishlock, T.W., Pethica, J.B. and Eydell, R.G. (2000) *Surf. Sci.* **445,** L47.
Gardiner, C.W. (1985) *Handbook of Stochastic Methods*, Springer-Verlag, New York.
González , J.E. and Ramirez-Pastor, A.J. (2002) *Physica A* **311,** 339.
Hill, T.L. (1956) *Statistical Mechanics*, McGraw-Hill, New York.
Jaroniec, M. and Bräuer, P. (1986) *Surf. Sci. Rep.* **6,** 65.
Jaroniec, M. and Madey, R. (1988) *Physical Adsorption on Heterogeneous Surfaces*, Elsevier, Amsterdam, The Netherlands.
Lopinski, G.P., Wayner, D.D.M. and Wolkow, R.A. (2000) *Nature (London)* **406,** 48.
Nazzarro, M. and Zgrablich, G. (2003) *Langmuir* **19,** 6737.
Nicholson, D. and Parsonage, N.G. (1982) *Computer Simulation and the Statistical Mechanics of Adsorption*, Academic Press, London.

Nieto, F. and Uebing, C. (1998) *Eur. Phys. J.* **B1,** 523.
Nitta, T., Kiriyama, H. and Shigeta, T. (1997) *Langmuir* **13,** 903.
Nitta, T., Kuro-oka, M. and Katayama, T. (1984) *J. Chem. Eng. Jpn.* **17,** 45.
Patrykiejew, A. (1993) *Langmuir* **9,** 2562.
Riccardo, J.L., Chade, M.A., Pereyra, V.D. and Zgrablich, G. (1992) *Langmuir* **8,** 1518.
Ripa, P. and Zgrablich, G. (1975) *J. Phys. Chem.* **79,** 2118.
Romá, F., Bulnes, F., Ramirez-Pastor, A.J. and Zgrablich, G. (2003) *J. Phys. Chem. Chem. Phys.* **5,** 3694.
Rudziński, W. and Everett, D.H. (1992) *Adsorption of Gases on Heterogeneous Surfaces*, Academic Press, London.
Rudziński, W., Steele, W.A. and Zgrablich, G. (1997) *Equilibria and Dynamics of Gas Adsorption on Heterogeneous Solid Surfaces*, Elsevier, Amsterdam, The Netherlands.
Steele, W.A. (1974) *The Interaction of Gases with Solid Surfaces*, Pergamon Press, Oxford, U.K.
Steele, W.A. (1999) *Langmuir* **15,** 6083.
Yang, M.X., Gracias, D.H., Jacobs, P.W. and Somorjai, G. (1998) *Langmuir* **14,** 1458.
Yeomans, J.M. (1992) *Statistical Mechanics of Phase Transitions*, Clarendon Press, Oxford, U.K.
Zgrablich, G., Mayagoitia, V., Rojas, F., Bulnes, F., Gonzalez, A.P., Nazzarro, M., Pereyra, V., Ramirez-Pastor, A.J., Riccardo, J.L. and Sapag, K. (1996a) *Langmuir* **12,** 129.
Zgrablich, G., Zuppa, C., Ciacera, M., Riccardo, J.L. and Steele, W.A. (1996b) *Surf. Sci.* **356,** 257.